Supporting Information

Unraveling A Trap-and-Trigger Mechanism in the pH-Sensitive Self-Assembly of Spider Silk Proteins

Jason A. Wallace[†] and Jana K. Shen[†,‡*]

[†]Department of Chemistry and Biochemistry, [‡] School of Chemical, Biological and Materials Engineering, University of Oklahoma, Norman, OK

[*]Corresponding author. Phone: (405) 325-0458; Fax: (405) 325-6111; E-mail: jana.k.shen@ou.edu.

Additional Simulation Details

Simulation protocol

Molecular dynamics simulations at pH conditions were run at ambient temperature and pressure using Hoover thermostat[1] and Langevin piston pressure coupling[2]. The SHAKE algorithm was applied to all hydrogen bonds and angles to allow a timestep of 2 fs . The electrostatic interactions were calculated using the particle-mesh Ewald summation. The van der Waals interactions were calculated with a switching function starting at 10Å and ending at 14 Å. The implicit-solvent model GBSW[3] was employed with a refined set of atomic radii[4] to define the dielectric boundary. The ionic strength in the GB calculation was set to 100 mM. The pH-REX protocol was enabled through a Perl package, MMTSB toolset[5], which provides an interface with the CHARMM program. To optimize the exchange frequency between neighboring pH replicas, trial 1-ns pH-REX simulations were carried out with pH conditions 0–10 with 1 pH unit intervals. The exchange success ratios were examined, and additional replicas were added at 0.5 pH unit intervals between replicas with exchange ratios below 20%. For monomer simulations, there were 14 replicas at pH values of 0.0, 1.0, 2.0, 2.5, 3.0, 3.5, 4.0, 4.5, 5.0, 6.0, 7.0, 8.0, 9.0, and 10.0. For the dimer simulation there were 17 replicas at pH values of 0.0, 1.0, 1.5, 2.0, 2.5, 3.0, 3.5, 4.0, 4.5, 5.0, 5.5, 6.0, 6.5, 7.0, 8.0, 9.0, and 10.0.

Poisson-Boltzmann calculations

Electrostatic potential maps were calculated using the Poisson-Boltzmann (PB) facility in the CHARMM program[6]. The atomic charges on the titratable residues at different pH conditions were set as the average charge calculated from the pH-REX titration simulation at the respective pH condition. The PB calculations used a salt concentration of 100 mM, a 1Å ion exclusion (Stern) layer, an internal dielectric constant of 4 and an external dielectric constant of 80. Electrostatic potential maps were rendered using the program VMD[7].

Error estimates

To estimate the uncertainty of the calculated pK_a values (fitting parameters k), we applied the well-known Monte Carlo "bootstrap" method[8]. The method comprises three steps: (1) generate a large number (we used 100) of independent bootstrap samples $S^*(i), i = 1...N$, where S represents the unprotonated fraction; (2) calculate the quantity of interest, e.g., the fitting parameter $k^*(i)$ for N bootstrap samples; and (3) calculate the standard deviation of the $k^*(i)$ values. For step (2) we assume that the probability of selecting a particular S value in each set S_i^* is given by a Gaussian distribution centered at $S^{\mathrm{final}}(\mathrm{pH})$ and having a standard deviation calculated by a block-averaging analysis[9,10] of the unprotonated fraction. The error associated with the resulting pH-dependent free energy of dimer dissociation was calculated by propagating the estimated error in calculated pK_a values.

Table S1: Calculated pK_a values in the unbound (monomer) and bound (dimer) states[a]

Residue	p$K_\mathrm{a}^{\mathrm{unbound}}$	p$K_\mathrm{a}^{\mathrm{bound}}$	ΔpK_a[b]
Monomer A			
His6	6.83 ± 0.07	6.88 ± 0.07	0.05 ± 0.10
Glu17	4.06 ± 0.02	4.10 ± 0.03	0.04 ± 0.04
Asp39	3.05 ± 0.05	1.31 ± 0.06	-1.74 ± 0.07
Asp40	4.11 ± 0.05	4.62 ± 0.04	0.51 ± 0.06
Glu79	4.42 ± 0.04	6.26 ± 0.05	1.84 ± 0.07
Glu84	4.40 ± 0.04	4.91 ± 0.06	0.51 ± 0.07
Glu85	3.92 ± 0.04	3.89 ± 0.04	-0.03 ± 0.05
Glu119	4.23 ± 0.05	6.12 ± 0.04	1.89 ± 0.05
Asp134	3.83 ± 0.05	3.55 ± 0.07	-0.28 ± 0.08
CT-Ala	3.35 ± 0.04	3.36 ± 0.04	0.01 ± 0.05
Monomer B			
His6	7.10 ± 0.04	7.73 ± 0.07	0.63 ± 0.08
Glu17	4.15 ± 0.05	4.15 ± 0.04	0.00 ± 0.06
Asp39	2.80 ± 0.04	2.03 ± 0.06	-0.77 ± 0.07
Asp40	4.19 ± 0.05	3.13 ± 0.10	-1.06 ± 0.11
Glu79	4.43 ± 0.05	6.73 ± 0.06	2.30 ± 0.08
Glu84	4.48 ± 0.07	4.70 ± 0.04	0.22 ± 0.08
Glu85	3.97 ± 0.04	3.88 ± 0.04	-0.09 ± 0.06
Glu119	4.32 ± 0.03	6.71 ± 0.05	2.39 ± 0.06
Asp134	4.22 ± 0.06	3.58 ± 0.04	-0.64 ± 0.07
CT-Ala	3.37 ± 0.03	3.73 ± 0.05	0.36 ± 0.06

[a] pK_a values determined by fitting the simulated unprotonated fractions to the Hill equation. Error bars are the standard deviation of 100 bootstrap trial fittings. [b] ΔpK_a = p$K_\mathrm{a}^{\mathrm{bound}}$ - p$K_\mathrm{a}^{\mathrm{unbound}}$
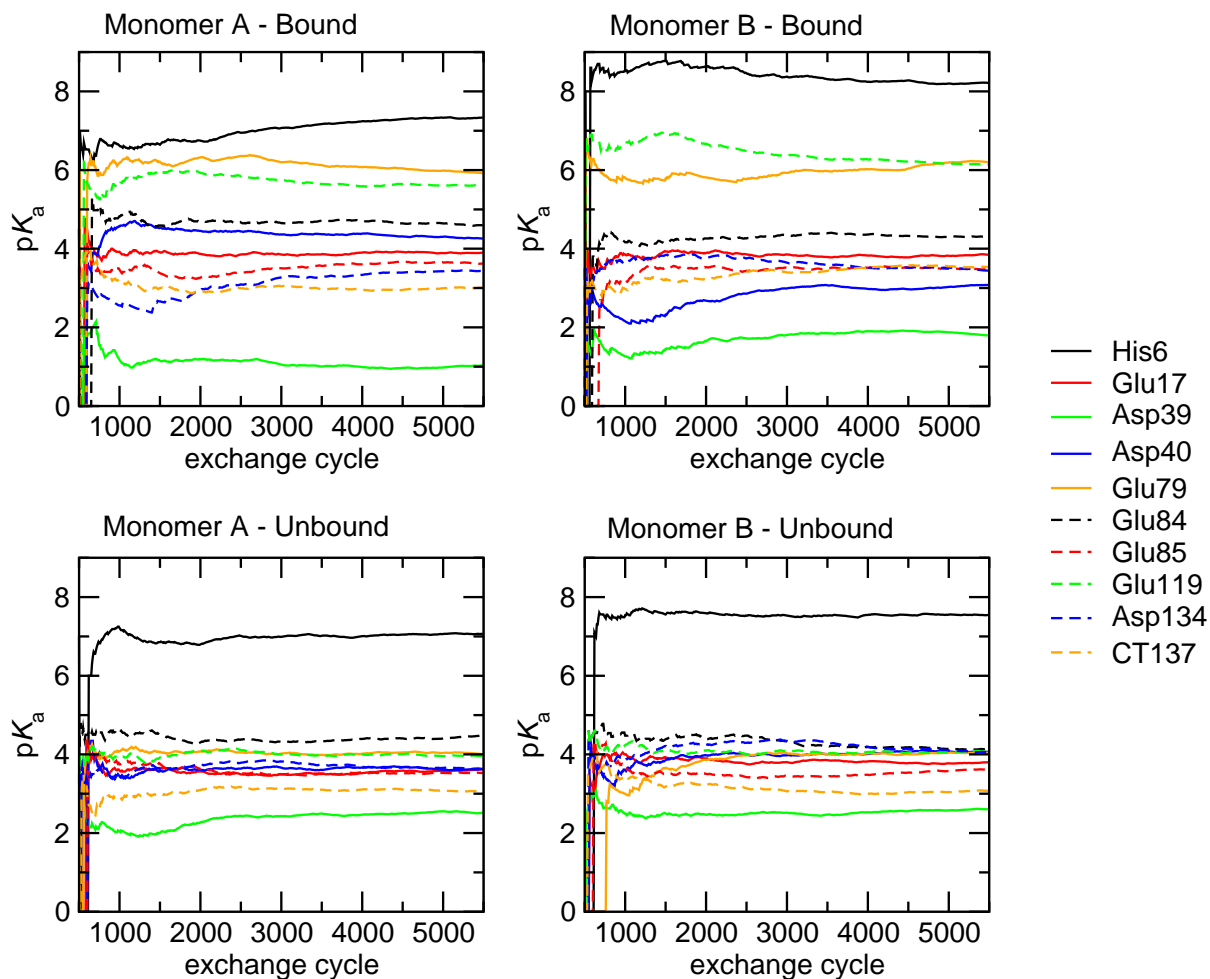Error bars are the standard deviation (σ) of 100 bootstrap trial fittings.

Figure S1: Running pK_a values estimated from the unprotonated fraction (S) at the pH value nearest the pK_a for all residues titrated.
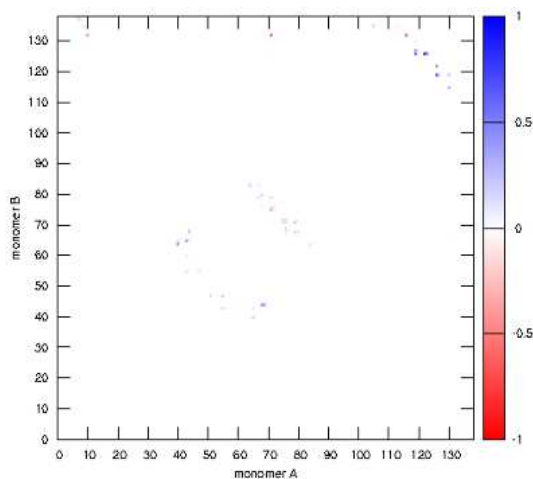

Figure S2: Difference (pH 4 less pH 8) contact probability map for the monomer-monomer interactions. Positive value indicates more probable contact at pH 4, while negative value indicates contact more probable contact at pH 8. Residues are considered to be in contact if the geometric centers of the sidechain heavy atoms are within 7Å.
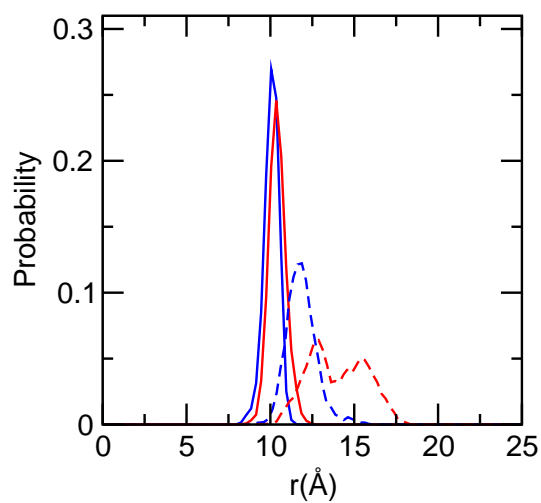
Figure S3: Probability distribution of the distance to the center-of-mass of the dimer from Glu79 (solid) and Glu119 (dashed) at pH 4 (blue) and pH 8 (red).
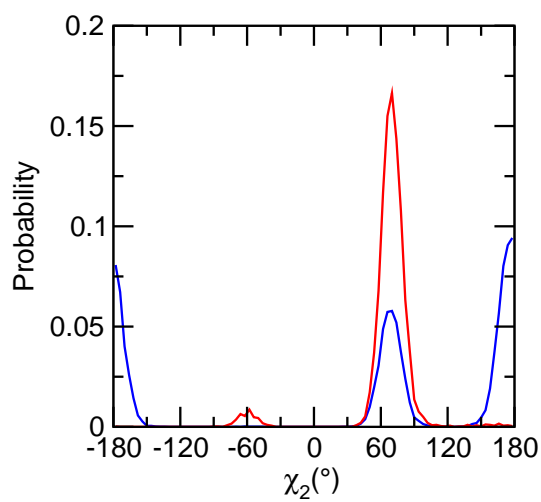

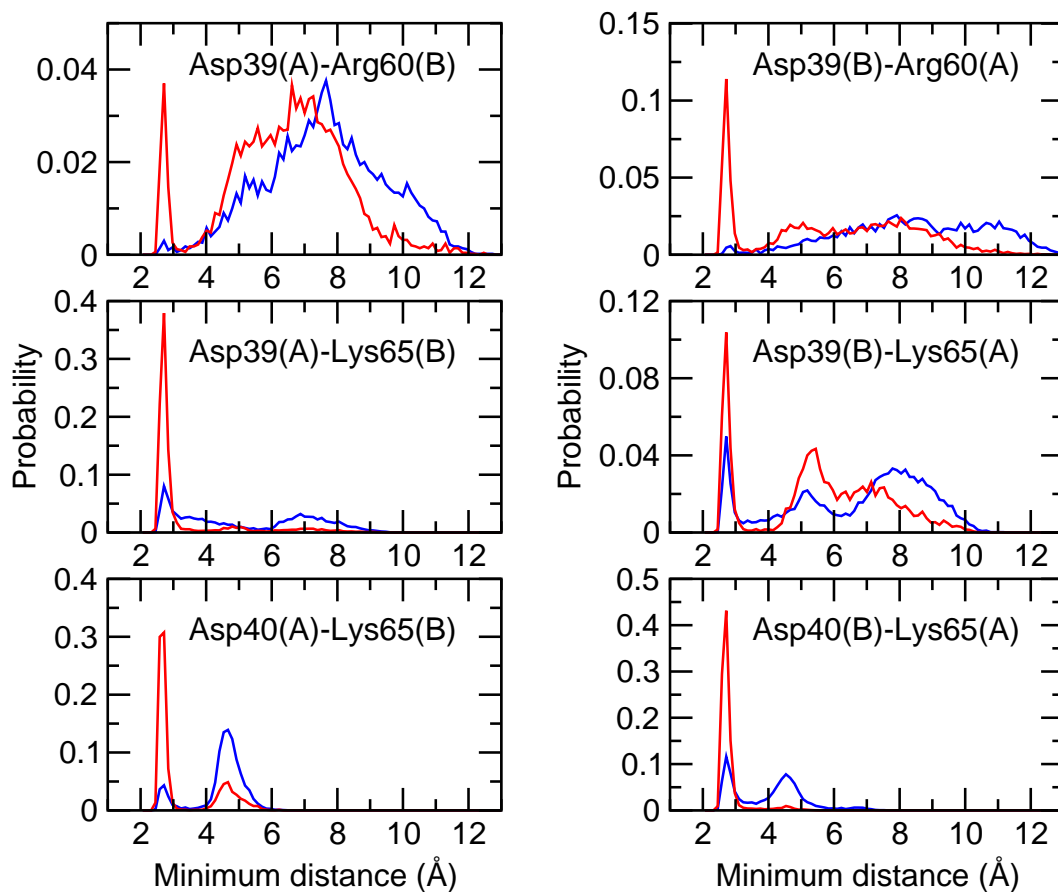Figure S4: Probability distribution of the χ_2 angle of Glu119 at pH 4 (blue) and pH 8 (red).

Figure S5: Salt-bridge interactions between Asp39, Asp40 and basic residues of the opposite subunit. Probability distribution of the minimum distance between heavy atoms in Asp39-Arg60, Asp39-Lys65 and Asp40-Lys65 when the acidic residue is fully deprotonated (red) and fully protonated (blue). The distribution for the pH condition The subunit is indicated in the parenthesis.

(1) Hoover, W. G. Canonical Dynamics: Equilibration Phase-Space Distributions. *Phys. Rev. A* **1985**, *31*, 1695–1697.

(2) Feller, S. E.; Zhang, Y.; Pastor, R. W.; Brooks, B. R. Constant Pressure Molecular Dynamics Simulation: The Langevin Piston Method. *J. Chem. Phys.* **1995**, *103*, 4613–4621.

(3) Im, W.; Lee, M. S.; Brooks, C. L.III *J. Comput. Chem.* **2003**, *24*, 1691–1702.

(4) Chen, J.; Im, W.; Brooks, C. L.III *J. Am. Chem. Soc.* **2006**, *128*, 3728–3736.

(5) Feig, M.; Karanicolas, J.; Brooks, C. L.III MMTSB Tool Set: Enhanced Sampling and Multiscale Modeling Methods for Applications in Structural Biology. *J. Mol. Graph. Model.* **2004**, *22*, 377–395.

(6) Brooks, B. R.; Brooks, C. L. III; MacKerell, A. D. Jr.; Nilsson, L.; Petrella, R.; Roux, B.; Won, Y.; Archontis, G.; Bartles, C.; Boresch, S. *et. al.* CHARMM: The Biomolecular Simulation Program. *J. Comput. Chem.* **2009**, *30*, 1545–1614.

(7) Humphrey, W.; Dalke, A.; Schulten, K. VMD: Visual Molecular Dynamics. *J. Mol. Graphics* **1996**, *14*, 33–38.

(8) Efron, B.; Tibshirani, R. Bootstrap Methods for Standard Errors, Confidence Intervals, and Other Measures of Statistical Accuracy. *Stat. Sci.* **1986**, *1*, 54–75.

(9) Flyvbjerg, H.; Petersen, H. G. Error Estimates on Averages of Correlated Data. *J. Chem. Phys.* **1989**, *91*, 461–466.

(10) Grossfield, A.; Zuckerman, D. M. Quantifying Uncertainty and Sampling Quality in Biomolecular Simulations. *Annu. Report Comput. Chem.* **2009**, *5*, 23–48.